Global Journal of Engineering and Technology Advances
eISSN: 2582-5003
Cross Ref DOI: 10.30574/gjeta
Journal homepage: https://gjeta.com/

(RESEARCH ARTICLE)

Check for updates

# Entropy generation in unsteady MHD convective flow past a flat porous oscillating plate with suction or injection

Akpabokigho L Panya [1, 2, *], Olufemi A Akinyemi [2] and Akindele M Okedoye [2, 3]

[1] *Department of Mathematics, College of Education, Warri, Delta State, Nigeria.*
[2] *Department of Mathematics, Federal University of Petroleum Resources, Effurun, Delta State, Nigeria.*
[3] *Department of Mathematics, Covenant University, Canaan Land, Ota, Ogun State, Nigeria.*

Global Journal of Engineering and Technology Advances, 2023, 14(02), 107–127

Publication history: Received on 08 January 2023; revised on 18 February 2023; accepted on 21 February 2023

Article DOI: https://doi.org/10.30574/gjeta.2023.14.2.0037

## Abstract

In this study, Entropy generation in MHD convective flow past a flat porous oscillating plate with suction or injection are presented for an unsteady, one-dimensional flow of a viscous incompressible fluid. The importance of Entropy generation is noticed in industrial and scientific fields including heat transfer in thermal systems which includes viscous dissipation, chemical reaction, mass transfer, heat transfer, and electrical conduction etc. The role of flow parameters like magnetic parameter, Radiation parameters, Grashof number, Heat generation/absorption, irreversibility distribution ratio on entropy generation are presented and elaborated through graphs. The obtained results reveal that for various values of Hartmann number, the entropy generation and Bejan number are increased, a larger radiation parameter increases the entropy generation and the Entropy generation due to viscous irreversibility decreases with the increase in Grashof number and Hartmann number.

**Keywords:** Porous media; MHD; Entropy generation; Unsteady flow: MSC 2020 Classification: 76S99; 76W99; 76M45; 76D99

## 1. Introduction

Fluid flow and heat transfer characteristics in porous medium is one of the fundamental types of research in engineering. It is a well-known issue that spawned its own academic's discipline. The concept is used in a wide range of fields, including applied sciences, petroleum and construction engineering, geosciences, biology and material sciences. Flow in porous medium and entropy generation has a significant commitment to current innovations and advanced applications. Fluid flow due to porous medium is of keen interest and are applied in fields like atomic waste archive, artificial dialysis, catalytic converters, gas turbine, improved oil recuperation, grain stockpiling, geo-energy production, and warm protection designing, etc. Menni et al. [1] report that these problems occur in barely all aspect of technological development as mentioned above. The flow through porous media is reported extensively by the following literature review by the studies Saffman [2], Hayatet al. [3] and Krishnamurthy et al. [4].

The fundamental concept of magnetohydrodynamics is that the magnetic effect can induce a current in electrically conductive fluid and consequently polarize the materials. Magnetohydrodynamics has various applications in several processes including plasmas, star formation, x-ray radiation, solar wind, tumor therapy, electrolytes, fusion and fission reactions, etc. Therefore, many researchers have paid their attention towards its study Sharma and Singh [5] have reported the unsteady MHD-free convective flow and heat transfer along a vertical porous plate with variable suction and internal heat generation. Singh and Gupta [6] have discussed the MHD-free convective flow of a viscous fluid through a porous medium bounded by an oscillating porous plate in slip flow regime with mass transfer. Haroun et al.

* Corresponding author: Akpabokigho L Panya

[7] examined the unsteady MHD mixed convection in a nanofluid due to a stretching/shrinking surface with suction/injection using the spectral relaxation method. Vaidya et al. [8] performed analysis of entropy generation and biomechanical investigation of MHD Jeffery fluid through a vertical non-uniform channel. Some studies regarding MHD flows in porous medium are reported by Ullah [9], Krishnamurthy [10], Abbas [11] and Makinde et al. [12].

Okedoye and Salawu [13] studied analytically the heat and mass transfer of unsteady MHD natural convective flow past a motioning plate with binary chemical reaction. Their results show amongst others that temperature is enhanced as the fluid angular velocity rises which leads to maximum temperature in the body of the liquid. while velocity decrease with a rise in the species reaction and reaction order. In another paper, Okedoye and Salawu [14] conducted a theoretical investigation on the flow of nonlinear magnetohydrodynamic (MHD), laminar, viscous, incompressible boundary layer fluid with thermal radiative heat transfer and variable properties past a stretching plate was carried out when the liquid is taken to be gray, absorbing, emitting but with non-scattering medium. The results shows that the parameters which enhanced the heat source terms decreased the fluid viscosity and caused increase in the flow rate, on the other hand, parameter that reduced heat source terms encouraged viscosity which resulted in retardation of the fluid velocity. An investigation into unsteady flow of heat and species transport through a porous medium in an infinite movable vertical permeable flat surface is considered was conducted by Okedoye and Salawu [15]. The impact of some pertinent flow terms revealed that the species boundary layer increases with a generative. Recently, Okedoye et al. [16] present their analysis on the transient double diffusion of a binary mixture in a porous moving flat device. their discussion revealed that a monotonically increase in the thermal diffusion is strongly impacted by an increasing value of heat generation and radiation throughout the flow regime. So also, MHD Darcy-Forchheimer Slip Flow in a Porous Medium with Variable Thermo-Physical Properties was presented by Panya et al. [17]. The results show that increasing the velocity slip parameter result in increase in velocity and Nusselt number whereas the concentration decreases in same case under specific condition.

With the advancement in industrial processes, entropy generation-EG is seen as appropriate solution to improve efficiency. Entropy generation-EG can be produced by several means for instance, heat transfer in thermal systems which includes viscous dissipation, chemical reaction, mass transfer, heat transfer, and electrical conduction. Entropy tells us in a way, the best we can do to avoid thermal energy losses. Bejan [18] was the first to introduce this concept by means of entropy generation minimization (EGM) also known as second law analysis and thermodynamics optimization. Bejan [19] analysed local entropy generation due to heat transfer and viscous effects for convective heat transfer in a channel. Qing et al. [20] examined entropy generation-EG on MHD flow of nanofluids over a porous permeable linear stretching or shrinking surface by using Casson fluid. The surface temperature of the stretching sheet was kept contact. Abiodun Ajibade et al. [21] investigate entropy generation under the effect of suction /injection between two infinite parallel porous plates as well as viscous dissipation. Shit et al. [22] looked at entropy generation on MHD flow and convective heat transfer in a porous medium of exponentially stretching surface saturated by nanofluids where they discovered that the Bejan number has strong impact on applied magnetic field, dissipation energy, thermal radiation and Biot number. Rashidi et al. [23] studied Entropy analysis of convective MHD flow of third grade non-Newtonian fluid over a stretching sheet, Farooq et al. [24] discussed the influence of transpiration and viscous dissipation on entropy flow over a nonlinear radially stretching disk. Nayak et al. [25] researched on the electro-magneto mixed convective flow of carbon-based nanoliquid with homogenous and heterogeneous chemical reactions. Entropy rate in MHD viscous liquid flow over stretchable sheet is reported by Khan et al. [26]. Bianco et al. [27] investigated the entropy generation of turbulent convective flow $Al_2O_3$ –water nanofluid in a tube under constant wall heat flux condition where they find out that the total entropy generation can be minimized for a low concentration of the particles. The influence of fluid viscosity on the entropy generation due to turbulent pipe flow heated from the pipe wall at constant temperature is investigated by Al-Zaharnah and Yilbas [28]. Some other studies regarding entropy generation due to heat transfer and fluid flows under various conditions are presented by Abbas et al. [29]; Tayebi et al. [30]; Avellaneda et al. [31]; Hayat et al. [32]; Ramesh et al. [33]; Waqas [34]; Khan et al. [35]; Sahin [36, 37]; and Makinde et al. [38]).

Most of the published analyses have been restricted, from a thermodynamic point of view, to only First-Law (of thermodynamics) analyses. To further gain more understanding on the study of entropy generation and its effects on convective flow, this paper examines entropy generation in unsteady MHD convective flow past a flat porous oscillating plate with suction or injection. In the present research, we investigate influence of various physical parameters on the behavior of velocity, temperature and concentration profile of the fluid, the influence of dissipation effect on thermal field and entropy generation, the behavior of reactive parameter on concentration and some dimensionless parameters are discussed in details.

## 2. Mathematical modelling

### 2.1. Flow and governing equations

Consider an unsteady one – dimensional convective flow of a viscous incompressible fluid with radiative heat transfer and chemical reaction past a flat plate moving through a binary mixture. Let the *x*-axis be taken along the plate in the direction of the flow and the y-axis be taken normal to it. A magnetic field of uniform strength $B_0$ is applied in the direction of flow and the temperature field is neglected. Initially, the plate and the fluid are at same temperature $T_w$ in a stationary condition with concentration level $C_w$ at all points. At time $t > 0$ the plate starts oscillating in its own plane with a velocity$U_0$. Its temperature is raised to $Tw$ and the concentration level at the plate is raised to $C_w$. The ambient condition is given by $\varphi_\infty$ (where $\varphi = \{u, T, C\}$) and the part associated with motion called, dynamic part $\varphi_d$ is given as $\varphi_d = \varphi - \varphi_\infty$. The suffix ∞ in the derivatives is omitted since it is a constant. The binary chemical reaction follows the one used by Boddington [42], Ogunseye and Okoya [43] and Okedoye and Ogunniyi [44].

The physical variables are functions of $y$ and $t$ only. Therefore, the only velocity component is in $y$ -direction. By above assumption, the continuity equation could be written as

$$\frac{\partial v}{\partial y} = 0 \tag{1}$$

Under the Boussinesq's approximation, the fluid momentum, energy and species equations in the neighborhood of the plate is described by the following respectively

$$\frac{\partial u}{\partial t} + v\frac{\partial u}{\partial y} = -\frac{1}{\rho}\frac{\partial p}{\partial x} + v\frac{\partial^2 u}{\partial y^2} + g\beta_T(T - T_\infty) + g\beta_C(C - C_\infty) - \frac{\sigma}{\rho}B_0^2 u \tag{2}$$

$$\rho C_p\left(\frac{\partial T}{\partial t} + v\frac{\partial T}{\partial y}\right) = k\frac{\partial^2 T}{\partial y^2} + \bar{Q}(T - T_\infty) - \frac{\partial q_r}{\partial y} \tag{3}$$

$$\frac{\partial C}{\partial t} + v\frac{\partial C}{\partial y} = D_f\frac{\partial^2 C}{\partial y^2} - R_A \tag{4}$$

Where $\bar{Q}$ is the heat of chemical reaction.
Using the Roseland approximation for radiative heat transfer and the Roseland approximation for diffusion, the expression for the radiative heat flux $q_r$ can be given as

$$q_r = \left(\frac{-4\sigma}{3k_s}\right)\left(\frac{\partial T^4}{\partial y}\right) \tag{5}$$

Here in Eq. (9), the parameters $\sigma$ and $k_s$ represent the Stefan Boltzmann constant and the Roseland mean absorption coefficient, respectively.

Now on assuming that the temperature differences within the fluid flow are sufficiently small, $T^4$ in Eq. (9) can be expressed as a linear function of $T_\infty$ ' using the Taylor series expansion. The Taylor series expansion of $T^4$about $T_\infty$ , after neglecting the higher order terms, takes the form

$$T^4 \cong 4T_\infty^3 T - 3T_\infty^4 \tag{6}$$

We employed chemical reaction of Arrhenius type of the *1st* order irreversible reaction given by,

$$R_A = k_r^2(T - T\infty)^r \exp\left(-\frac{E_a}{R_G T}\right)(C - C_\infty) \tag{7}$$

Where $k_r$ is the reactivity of chemical reaction defined by frequency of collision $\omega$ and orientation factor $p$ as $k_r = k_r(\omega, p) = \omega p$, $R_G$ is the universal gas constant.

The appropriate initial and boundary conditions relevant to the problem are

$$\left.\begin{array}{l} t \le 0: u = U_0, v = v_w(t), T = T_w, C = C_w \ \forall y \\ t > 0: \begin{cases} u = U_1, T = T_w + A_1 e^{i\omega t}, C = C_w + A_2 e^{i\omega t}, y = 0 \\ u \to U(t), T \to T_\infty, C \to C_\infty \ as \ y \to \infty \end{cases} \end{array}\right\} \tag{8}$$

where $U_0$ is the plate characteristic velocity. $A_1, A_2 > 0$ *and* $A_1 = (T_w - T_\infty), A_2 = (C_w - C_\infty)$.

The stream velocity is given by

$$U(t) = 1 + \epsilon e^{i\omega t}$$

At free stream,

$$u \rightarrow U, T \rightarrow T_{\infty},, C \rightarrow C_{\infty}$$

while at time $y = 0$, the suction/blowing is a function free stream given as

$$v(t,0) = -v_0(1 + \epsilon e^{i\omega t}) \tag{9}$$

$v_0(> 0)$ is the suction velocity and $v_0(< 0)$ is the blowing velocity.

We now define conveniently the following dimensionless quantities;

$$y = \frac{vy'}{v_0}, v' = \frac{v}{v_0}, u' = \frac{u}{U_0}, t' = \frac{tv_0^2}{4\nu}, U' = \frac{U}{U_0}, \omega' = \frac{4\omega\nu}{v_0^2}, V = \frac{U_1}{U_0}$$
$$\theta(y,t) = \left(\frac{E_a}{R_G T_{\infty}^2}\right)(T - T_{\infty}) = \frac{T - T_{\infty}}{\epsilon T_{\infty}}, \qquad \emptyset(y,t) = \frac{C - C_{\infty}}{C_w - C_{\infty}} \tag{10}$$

Following Messiha [45], Equation (5) on integration becomes

$$v(t,y) = constant$$

At $t = 0$,

$$v(t,y) = v_w(t)$$

Using equation (13)

$$\Rightarrow v(t,y) = -v_0(1 + \epsilon e^{i\omega t}) \tag{11}$$

At free stream, u → U, T → T∞, C → C∞, thus from equation (6)

$$-\frac{1}{\rho}\frac{\partial p}{\partial x} = \frac{\partial U}{\partial t} = \frac{\partial}{\partial t}(1 + \epsilon e^{i\omega t})$$
$$-\frac{1}{\rho}\frac{\partial p}{\partial x} = \frac{\partial U}{\partial t} + \frac{\sigma}{\rho}B_0^2 U \tag{12}$$

Using the equations (9)-(11), (15) and (16), equations (6)-(8) after dropping primes becomes

$$\frac{1}{4}\frac{\partial u}{\partial t} - v_0(1 + \epsilon e^{i\omega t})\frac{\partial u}{\partial y} = \epsilon\left(\frac{i\omega}{4} - Ha\right)e^{i\omega t} + \frac{\partial^2 u}{\partial y^2} + Gr(N\theta + \phi) - H_a(u - 1) \tag{13}$$

$$\frac{1}{4}\frac{\partial \theta}{\partial t} - v_0(1 + \epsilon e^{i\omega t})\frac{\partial \theta}{\partial y} = \left(\frac{1 + \alpha}{Pr}\right)\frac{\partial^2 \theta}{\partial y^2} + \beta\theta \tag{14}$$

$$\frac{1}{4}\frac{\partial \phi}{\partial t} - v_0(1 + \epsilon e^{i\omega t})\frac{\partial \phi}{\partial y} = \frac{1}{Sc}\frac{\partial^2 \phi}{\partial y^2} - \epsilon\lambda\phi e^{\frac{\theta}{1+\epsilon\theta}} \tag{15}$$

Where $Ha, Gr, N, \alpha, \beta, Pr, Sc, \lambda$ and $n$ are the magnetic parameter, Grashof number, radiation parameter, heat generation/absorption, Prandtl and Schmidt numbers, reactivity parameter and $n \in \mathbb{Z}^+$ δ respectively.

The non-dimensional parameters governing the flow are define as

$$Ha = \frac{\sigma B_0^2 \nu}{v_0^2}, Gr = \frac{\nu g\beta_c(C_w - C_{\infty})}{U_0 v_0^2}, N = \frac{\epsilon g\beta_t T_{\infty}}{\beta_c(C_w - C_{\infty})}, \alpha = \frac{16}{3}\frac{T_{\infty}^3 \nu^2}{3kk_s},$$
$$\beta = \frac{\nu Q}{\rho c_p v_0^2}, Pr = \frac{\mu c_p}{k}, \qquad Sc = \frac{D_f}{\mu}, \lambda = k_r \epsilon^{n-1}\frac{T_{\infty}^n e^{\frac{1}{\epsilon}}\nu^2}{D_f v_0^2}$$

And the corresponding initial-boundary condition (12) becomes

$$t \geq 0: \begin{cases} y = 0 : u = V, \theta = 1 + e^{i\omega t}, & \emptyset = 1 + e^{i\omega t} \\ y \rightarrow \infty : u \rightarrow U, \theta \rightarrow 0, & \emptyset \rightarrow 0 \end{cases} \tag{17}$$

### 2.2. Entropy generation for convective heat and mass transfer

The second law of thermodynamics states that the change in entropy for a given system can be written as the sum of two terms des and dis. The first is the entropy change due to exchange of matter and energy with the exterior, the second is the entropy due to "uncompensated transformations", the entropy produced by the irreversible processes in the interior of the system (Hirschfelder [39] and Prigogine [40]):

$$ds = d_e s + d_i s \tag{17}$$

where:

$d_i s = 0$ for reversible processes

$d_i s > 0$ for irreversible processes

The entropy generation per unit time and volume, called local entropy generation rate is given by:

$$\Gamma = \frac{d_i s}{dt} \geq 0 \tag{18}$$

In convective heat and mass transfer and MHD flows, irreversibility arises due to viscous, heat and mass transfer effects. The entropy generation rate is expressed as the sum of contributions due to viscus, thermal and diffusive effects, and thus it depends functionally on the local values of temperature, velocity and concentration in the domain of interest. According to Bejan [6] the characteristics entropy transfer rate is given by

$$\Gamma_0 = k\left(\frac{\Delta T}{LT_0}\right)^2 \tag{19}$$

Where $k, L, T_0$ and $\Delta T$ are respectively, the thermal conductivity, the characteristics length of the enclosure, a reference temperature and a reference temperature difference.
Mourad et al [41], give two-dimensional entropy generation rate as

$$\begin{aligned}\Gamma = \frac{\mu}{T_0}\left[2\left(\frac{\partial u}{\partial x}\right)^2 + 2\left(\frac{\partial v}{\partial x}\right)^2 + \left(\frac{\partial v}{\partial x} + \frac{\partial u}{\partial y}\right)^2\right] + \frac{k}{T_0^2}\left[\left(\frac{\partial T}{\partial x}\right)^2 + \left(\frac{\partial T}{\partial y}\right)^2\right] \\ + \frac{RD}{C_0}\left[\left(\frac{\partial C}{\partial x}\right)^2 + \left(\frac{\partial C}{\partial y}\right)^2\right] + \frac{RD}{T_0}\left[\left(\frac{\partial T}{\partial x}\right)\left(\frac{\partial C}{\partial x}\right) + \left(\frac{\partial T}{\partial y}\right)\left(\frac{\partial C}{\partial y}\right)\right]\end{aligned} \tag{20}$$

Where $C_0$ and $T_0$ are respectively the reference concentration and temperature, which are in our case, the bulk concentration and the bulk temperature.

According to the equation (4), it is clear that the numerical calculation of the local entropy generation rate in a thermodynamics system requires the knowledge of the velocity, temperature and concentration fields in the system.

## 3. Method of solution

To solve equations (17) - (19) with the initial boundary conditions (20), perturbation in the neighborhood of $\epsilon$ is used, similar to the one used by Lighthill [46] and Okedoye and Ogunniyi [44]. The Velocity, specie concentration and temperature fields are given by the expressions

$$\begin{aligned} u(y,t) &= f_0(y) + e^{i\omega t} f_1(y), \\ \phi(y,t) &= h_0(y) + e^{i\omega t} h_1(y), \\ \theta(y,t) &= g_0(y) + e^{i\omega t} g_1(y). \end{aligned} \tag{21}$$

Substituting equations (17) into equation (15) - (16), separating the harmonic and non-harmonic terms and neglecting the coefficient of 2, we have

### 3.1. Mean Velocity, Temperature and Chemical Specie

$$f_0'' + v_0 f_0' - Haf_0 = -Gr(Ng_0 + h_0) - Ha \tag{22}$$

$$g_0'' + \frac{Prv_0}{1+\alpha} g_0' + \frac{Pr\beta}{1+\alpha} g_0 = 0, \tag{23}$$

$$h_0'' + Scv_0 h_0' - \varepsilon\lambda Sch_0 (g_0)^n e^{g_0} = 0, \tag{24}$$

With boundary conditions

$$\begin{aligned} y = 0 &: f_0 = V, g_0 = 1, h_0 = 1, \\ y \to \infty &: f_0 \to 0, g_0 \to 0, h_0 \to 0\,. \end{aligned} \tag{25}$$

*Oscillatory part of the Velocity, Temperature and Chemical Specie;*

$$f_1'' + v_0 f_1' - \left(Ha + \frac{i\cdot\omega}{4}\right) f_1 - \left(Ha - \frac{i\cdot\omega}{4}\right) = -v_0 f_0' - Gr(Ng_1 + h_1) \tag{26}$$

$$g_1'' + \frac{Prv_0}{1+\alpha} g_1' + \frac{Pr}{1+\alpha}\left(\beta - \frac{i\omega}{4}\right) g_1 = -\frac{Prv_0}{1+\alpha} g_0 \tag{27}$$

$$h_1'' + Scv_0 h_1' - \lambda Sch_1 \left(g_1 (g_0^n + n g_0^{n-1}) e^{g_0} - \frac{i\omega}{4}\right) = -v_0 h_0' \tag{28}$$

With boundary conditions

$$\begin{aligned} y = 0 &: f_1 = 0, g_1 = 1, h_1 = 1, \\ y \to \infty &: f_1 \to 0, g_1 \to 0, h_1 \to 0\,. \end{aligned} \tag{29}$$

From equation (24), we write

$$h_0'' + Scv_0 h_0' = \varepsilon\lambda Sch_0 (g_0)^n e^{g_0}$$

right hand side of above is expressed as follows

$$\varepsilon\lambda Sch_0 (g_0)^n e^{g_0} = \varepsilon\lambda Sch_0 (e^{-my})^n \sum_{r=0}^{k} \frac{1}{r!} g_0^r$$

We apply perturbation technique to equations (18), (20), (22) and (25) as the case maybe such as equation (20) which under this discussion becomes

$$h_0'' + Scv_0h_0' = \varepsilon\lambda Sch_0\sum_{r=0}^{k}\frac{1}{r!}e^{-m(n+r)y} \tag{30}$$

Let

$$h_0'' + Scv_0h_0' = 0, h_0(0) = 1, h(y) \to 0 \; as \; y \to \infty \tag{31}$$

The solution of (31) is

$$h_0(y) = e^{-S_cv_0y} \tag{32}$$

We assume that (32) is a small perturbation to the solution of (31), that is

$$h_0(y) = e^{-S_cv_0y} + \varepsilon\gamma_0(y) + O(\varepsilon^2) \tag{33}$$

The function $\gamma_0(y)$ need to be determined. The initial condition for $\gamma_0(y)$ is found as follows

$$h_0(0) = 1 + \varepsilon\gamma_0(0) + O(\varepsilon^2) = 1$$
$$\Longrightarrow \gamma_0(0) = 0$$

Also,

$$h_0(y) = e^{-S_cv_0y} + \varepsilon\gamma_0(y) + O(\varepsilon^2) \longrightarrow 0 \; as \; y \longrightarrow \infty$$
$$\Longrightarrow \gamma_0(y) \longrightarrow 0 \; as \; y \longrightarrow \infty$$

Now substitute (33) into (30)

$$\gamma_0'' + Scv_0\gamma_0' = \lambda Sce^{-S_cv_0y}\sum_{r=0}^{k}\frac{1}{r!}e^{-m(n+r)y} = \lambda Sc\sum_{r=0}^{k}\frac{1}{r!}e^{-[m(n+r)+S_cv_0]y}$$

$$\gamma_0'' + Scv_0\gamma_0' = \lambda Sc\sum_{r=0}^{k}\frac{1}{r!}e^{-[m(n+r)+S_cv_0]y} \tag{34}$$

The solution of (34) is

$$\gamma_0(y) = a_3e^{-S_cv_0y} + \sum_{r=0}^{k}\frac{a_4}{r!}e^{-[m(n+r)+S_cv_0]y} \tag{35}$$

Where

$$a_3 = -\sum_{r=0}^{k}\frac{a_4}{r!}, a_4 = -\frac{\lambda Sc}{m(n+r)(m(n+r)+S_cv_0)}$$

Substitute (35) into (33), we have the solution $h_0(y)$ as

$$h_0(y) = (1+\varepsilon a_3)e^{-S_cv_0y} + \varepsilon\sum_{r=0}^{k}\frac{a_4}{r!}e^{-[m(n+r)+S_cv_0]y}$$

Following similar perturbation procedures, the solutions of equations (22) - (24) and (26) - (28) under the boundary conditions (25) and (29) respectively are

$$g_0(y) = e^{-my} \tag{36}$$

$$h_0(y) = (1+\varepsilon a_3)e^{-S_cv_0y} + \varepsilon\sum_{r=0}^{k}\frac{a_4}{r!}e^{-[m(n+r)+S_cv_0]y} \tag{37}$$

$$f_0(y) = a_5e^{-n_1y} + a_6e^{-my} + a_7e^{-S_cv_0y} + \sum_{r=0}^{k}\frac{a_8a_4}{r!}e^{-[m(n+r)+S_cv_0]y} - 1 \tag{38}$$

$$g_1(y) = a_1e^{-m_1y} + a_2e^{-my} \tag{39}$$

$$\begin{aligned} h_1(y) = e^{-S_cv_0y} + \varepsilon\Bigg\{ & a_{15}e^{-S_cv_0y} + \sum_{r=0}^{k}\frac{1}{r!}a_9e^{-(m_1+(n+r)m+S_cv_0)y} + \sum_{r=0}^{k}\frac{1}{r!}a_{10}e^{-(m_1+(n+r-1)m+S_cv_0)y} \\ & + \sum_{r=0}^{k}\frac{1}{r!}a_{11}e^{-(m(n+r+1)+S_cv_0)y} + \sum_{r=0}^{k}\frac{1}{r!}a_{12}e^{-((n+r)m+S_cv_0)y} + \sum_{r=0}^{k}\frac{a_{13}}{r!}e^{-[m(n+r)+S_cv_0]y} + a_{14}y\,e^{-S_cv_0y}\Bigg\} \end{aligned} \tag{40}$$

$$\begin{aligned} f_1(y) = {} & a_{16}e^{-n_1y} + a_{17}e^{-my} + (a_{18}+a_{19}y)e^{-S_cv_0y} + a_{20}e^{-m_1y} - \sum_{r=0}^{k}\frac{1}{r!}a_{21}e^{-(m_1+(n+r)m+S_cv_0)y} \\ & - \sum_{r=0}^{k}\frac{1}{r!}a_{22}e^{-(m_1+(n+r-1)m+S_cv_0)y} - \sum_{r=0}^{k}\frac{1}{r!}a_{23}e^{-[m(n+r)+S_cv_0]y} + a_{24}a_{25}e^{-\tau y} + \end{aligned} \tag{41}$$

It should be noted that the analysis of $e^{g_0}$ is found to be equivalent to

$$\sum_{r=0}^{k} \frac{1}{r!} g_0^r \text{ as } k \geq 3$$

That is

$$e^{g_0} \equiv \sum_{r=0}^{k} \frac{1}{r!} g_0^r \text{ as } k \geq 3 \tag{42}$$

To validate the equivalence of (36), we plot the LHS and RHS on the same axis at $k = 3$. The result at $Pr = 0.71, v_0 = 0.1,\ \alpha = -0.1,\ \beta = -0.1$ is shown below:

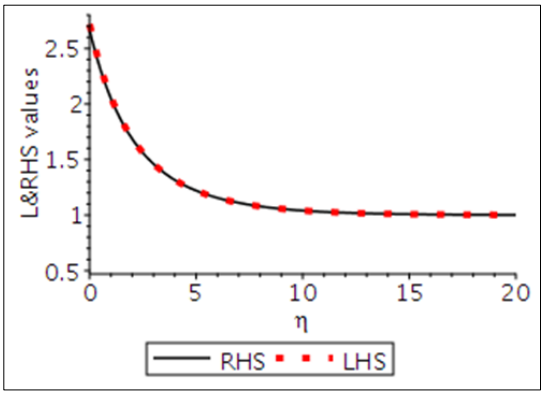


**Figure 1** Graph showing $\boldsymbol{LHS = e^{g_0}}$ and $\boldsymbol{RHS = \sum_{r=0}^{k} \frac{1}{r!} g_0^r}$

The above solution requires that

$$\frac{Prv_0 - \sqrt{Pr^2 v_0^2 - 4Pr(1+\alpha)(\beta - \frac{i\omega}{4})}}{2(1+\alpha)} \geq 0$$
$$\Rightarrow \alpha < -1 \,\&\, \beta \leq \frac{i\omega}{4} \text{ or } \alpha > -1 \,\&\, \beta \geq \frac{i\omega}{4}$$

Provided

$$\alpha < -1 \,\&\, \beta < 0 \; or \; \alpha > -1 \,\&\, \beta > 0$$

and

$$m \in \Re \Rightarrow Pr^2 v_0^2 - 4Pr(1+\alpha)\beta \geq 0 \Rightarrow \beta \leq \frac{Prv_0^2}{4(1+\alpha)}$$

On substituting equations (32) - (37) into (17), the $2-$*dimensional* expression for the velocity, concentration and temperature distribution are

$$\begin{aligned} u(y,t) = -1 + a_5 e^{-n_1 y} + a_6 e^{-my} + a_7 e^{-S_c v_0 y} + \sum_{r=0}^{k} \frac{a_8 a_4}{r!} e^{-[m(n+r)+S_c v_0]y} + \epsilon e^{i\omega t}(a_{25} e^{-\tau y} \\ + a_{16} e^{-n_1 y} + a_{17} e^{-my} + (a_{18} + a_{19} y) e^{-S_c v_0 y} + a_{20} e^{-m_1 y} - \sum_{r=0}^{k} \frac{1}{r!} a_{21} e^{-(m_1+(n+r)m+S_c v_0)y} \\ - \sum_{r=0}^{k} \frac{1}{r!} a_{22} e^{-(m_1+(n+r-1)m+S_c v_0)y} - \sum_{r=0}^{k} \frac{1}{r!} a_{23} e^{-[m(n+r)+S_c v_0]y} + a_{24} \Big) \end{aligned} \tag{43}$$

$$\begin{aligned} \phi(y,t) = (1+\varepsilon a_3) e^{-S_c v_0 y} + \varepsilon \sum_{r=0}^{k} \frac{a_4}{r!} e^{-[m(n+r)+S_c v_0]y} + \epsilon e^{i\omega t} \Bigg( e^{-S_c v_0 y} + \varepsilon \Bigg\{ \sum_{r=0}^{k} \frac{1}{r!} a_9 e^{-(m_1+(n+r)m+S_c v_0)y} \\ + \sum_{r=0}^{k} \frac{1}{r!} a_{10} e^{-(m_1+(n+r-1)m+S_c v_0)y} + \sum_{r=0}^{k} \frac{1}{r!} a_{11} e^{-(m(n+r+1)+S_c v_0)y} + \sum_{r=0}^{k} \frac{1}{r!} a_{12} e^{-((n+r)m+S_c v_0)y} \\ + \sum_{r=0}^{k} \frac{a_{13}}{r!} e^{-[m(n+r)+S_c v_0]y} + a_{14} y\, e^{-S_c v_0 y} + a_{15} e^{-S_c v_0 y} \Bigg\} \Bigg) \end{aligned} \tag{44}$$

$$\theta(y,t) = e^{-my} + \epsilon e^{i\omega t}(a_1 e^{-m_1 y} + a_2 e^{-my}) \tag{45}$$

## 4. Entropy generation for convective heat and mass transfer

### 4.1. Dimensionless entropy generation

As mentioned, in convective heat and mass transfer and for a non-reactive mixture, irreversibility arises due to the heat transfer, the viscous effects and the mass transfer. The entropy generation rate is expressed as the sum of contributions due to thermal, viscous and diffusive effects, and thus it depends functionally on the local values of temperature, velocity and concentration in the domain of interest. Many authors, namely, Shohel and Roydon [47] and Tasnim and Shohel [48] gave a dimensionless form of the local entropy generation in convective heat transfer, which is a ratio between the local entropy generation rate and a characteristic entropy transfer rate given by (3).

Using (43)-(45) in (4), we thus have the dimensionless form of local entropy generation is express as,

$$\Gamma = \left(\frac{\partial\theta}{\partial y'}\right)^2 + \frac{2\mu}{T_\infty k}\left(\frac{R_G T_\infty}{E_a}\right)^{-2} {U_\infty}^2 \left(\frac{\partial u'}{\partial y'}\right)^2 + \frac{1}{k}\left(\frac{R_G T_\infty}{E_a}\right)^{-2} \frac{RD}{C_\infty}\left((C_w - C_\infty)\right)^2 \left(\frac{\partial\phi}{\partial y'}\right)^2 + \frac{1}{k}\left(\frac{R_G T_\infty}{E_a}\right)^{-1} \frac{RD}{T_\infty}\left((C_w - C_\infty)\right)\left(\frac{\partial T}{\partial y'}\right)\left(\frac{\partial\phi}{\partial y'}\right) \tag{46}$$

The dimensionless total entropy generation is the integral over the system volume of the dimensionless local entropy generation. In our case here, using equation (46), total entropy is given by summation of all local entropy stated as

$$E_G = \underbrace{\left(\frac{\partial\theta}{\partial y}\right)^2}_{\text{Thermal irreversibility}} + \underbrace{\delta_1\left(\frac{\partial u}{\partial y}\right)^2}_{\text{Viscous irreversibility}} + \underbrace{\delta_2\left(\frac{\partial\phi}{\partial y}\right)^2 + \delta_3\left(\frac{\partial\theta}{\partial y}\right)\left(\frac{\partial\phi}{\partial y}\right)}_{\text{Diffusive irreversibility}} \tag{47}$$

Dimensionless terms denoted $\delta_i$, $(1 \le i \le 3)$ in equation (47) are called irreversibility distribution ratios, are given by:

$$\delta_1 = \frac{2U_\infty^2\mu}{T_\infty k}\left(\frac{E_a}{R_g T_\infty^2}\right)^2, \delta_2 = \frac{RD}{kC_\infty}\left(\frac{E_a\Delta C_\infty}{R_g T_\infty^2}\right)^2, \delta_3 = \frac{RD}{k}\frac{E_a\Delta C_\infty}{R_G T_\infty^2}$$

We define

$$\Gamma_{\mathrm{n},\theta} = \left(\frac{\partial\theta}{\partial y}\right)^2, \Gamma_{\mathrm{n,u}} = \delta_1\left(\frac{\partial u}{\partial y}\right)^2, \Gamma_{\mathrm{n},\phi} = \delta_2\left(\frac{\partial\phi}{\partial y}\right)^2, \Gamma_{\mathrm{n},\tau} = \delta_3\left(\frac{\partial\theta}{\partial y}\right)\left(\frac{\partial\phi}{\partial y}\right) \tag{48}$$

It is quite essential to calculate the significant input of each source of entropy production in a system, in view of this, the Bejan number describes the proportion of the entropy production by heat transfer to the total proportion as represented in equation (47) or (48),

$$Be = \frac{\Gamma_{\mathrm{n},\theta}}{E_G} = \frac{\Gamma_{\mathrm{n},\theta}}{\Gamma_{\mathrm{n},\theta} + \Gamma_{\mathrm{n,u}} + \Gamma_{\mathrm{n,d}}} \tag{49}$$

It is important to note that the entropy generation due to diffusion ($\Gamma_{\mathrm{n,d}} = \Gamma_{\mathrm{n},\phi} + \Gamma_{\mathrm{n},\tau}$) is the sum of a pure term ($\Gamma_{\mathrm{n},\phi}$) which involves concentration gradient only and a crossed term ($\Gamma_{\mathrm{n},\tau}$) with both thermal and concentration gradients. Therefore, a coupling effect between thermal gradient and concentration gradient can be shown in the expression of the entropy generation, whereas this coupling effect was neglected in the energy and specie conservation equations (Soret and Dufour effects) and also in the mass diffusion flux equation (first Fick's law). Bejan number ranges from 0 to 1. Accordingly, $Be \cong 1$ is the limit at which the heat transfer irreversibility dominates, $Be \cong 0$ is the opposite limit at which the irreversibility is dominated by fluid friction effects, and $Be = 1/2$ is the case in which the heat transfer and fluid friction entropy generation rates are equal.

Using (43)-(45) in (48), after some algebraic manipulations the results of entropy generation due to thermal, diffusion and viscous irreversibility are shown in the figure below.

$$\begin{aligned}\Gamma_{\mathrm{n},\theta} &= \Re\left((me^{-my} + \epsilon A)^2 - B^2 + 2IB(me^{-my} + \epsilon A)\right) \\ &= (me^{-my} + \epsilon A)^2 - B^2\end{aligned} \tag{50}$$

$$\begin{aligned}\Gamma_{\mathrm{n,u}} &= \Re\left(\delta_1\left(G^2 - 2\epsilon FG + \epsilon^2(F^2 - E^2) + 2I\epsilon E(G - \epsilon F)\right)\right) \\ &= \delta_1\left(G^2 - 2\epsilon FG + \epsilon^2(F^2 - E^2)\right)\end{aligned} \tag{51}$$

$$\Gamma_{\mathrm{n,d}} = \Re\left(\delta_2(K^2 - P^2 + 2IKP) + \delta_3(\alpha + I\beta)\right) = \delta_2(K^2 - P^2) + \delta_3\alpha \tag{52}$$

Thus,

$$\Gamma = \underbrace{(me^{-my} + \epsilon A)^2 - B^2 + 2IB(me^{-my} + \epsilon A)}_{\text{Thermal irreversibility}} + \underbrace{\delta_1\left(G^2 - 2\,\epsilon FG + \epsilon^2(F^2 - E^2) + 2I\epsilon\, E(G - \epsilon F)\right)}_{\text{Viscous irreversibility}} + \underbrace{\delta_2(K^2 - P^2 + 2IKP) + \delta_3(\alpha + I\beta)}_{\text{Diffusive irreversibility}} \tag{53}$$

Hence, total entropy generated is expressed as

$$E_G = \Re(\Gamma) = (me^{-my} + \epsilon A)^2 - B^2 + \delta_1\left(G^2 - 2\,\epsilon FG + \epsilon^2(F^2 - E^2)\right) + \delta_2(K^2 - P^2) + \delta_3\alpha \tag{54}$$

By equation (49), Bejan number is then given as

$$Be = \Re\left(\frac{(me^{-my} + \epsilon A)^2 - B^2 + 2IB(me^{-my} + \epsilon A)}{\left((me^{-my} + \epsilon A)^2 - B^2 + 2IB(me^{-my} + \epsilon A) + \delta_1\left(G^2 - 2\,\epsilon FG + \epsilon^2(F^2 - E^2) + 2I\epsilon\, E(G - \epsilon F)\right) + \delta_2(K^2 - P^2 + 2IKP) + \delta_3(\alpha + I\beta)\right)}\right) = \Re\left(\frac{a + bI}{c + Id}\right) = \frac{ac + bd}{c^2 + d^2} \tag{55}$$

where

$$A = \left((c_3m_2 - c_4m_3)\cos(m_2y + \omega t) - (c_4m_2 + c_3m_3)\sin(m_2y + \omega t)\right)e^{-m_2y} + c_1me^{-my}$$

$$B = \left((c_3m_2 - c_4m_3)\sin(m_2y + \omega t) + (c_4m_2 + c_3m_3)\cos(m_2y + \omega t)\right)e^{-m_2y} - c_2me^{-my}$$

$$E = c_8me^{-my} + (\tau_1c_{23}(-\tau_2c_{24})\cos\tau_2y - (\tau_1c_{24} + \tau_2c_{23})\sin\tau_2y)e^{-\tau_1y} + n_1a_{16}e^{-n_1y} + c_7me^{-my} + \left((c_9 + c_{11}y)S_cv_0 - c_{11}\right)e^{-S_cv_0y} - \sum_{r=0}^{k}\frac{1}{r!}c_{19}a_{33}e^{-a_{33}y} + \left((m_2c_{13} - m_3c_{14})\cos m_3y - (m_2c_{14} + m_3c_{13})\sin m_3y\right)e^{-m_2y} - \sum_{r=0}^{k}\frac{1}{r!}\left((a_{31}c_{15} - m_3c_{16})\cos m_3y - (a_{31}c_{16} - m_3c_{15})\sin m_3y\right)e^{-a_{31}y} - \sum_{r=0}^{k}\frac{1}{r!}\left(((a_{32}c_{17} - m_3c_{18})\cos m_3y - (a_{32}c_{18} + m_3c_{17})\sin m_3y\right)e^{-a_{32}y}\right)$$

$$F = \left((c_{10} + c_{12}y)S_cv_0 - c_{12}\right)e^{-S_cv_0y} - \sum_{r=0}^{k}\frac{1}{r!}c_{20}a_{33}e^{-a_{33}y} + (m_2c_{13} - m_3c_{14})\sin m_3y + (m_2c_{14} + m_3c_{13})\cos m_3y)e^{-m_2y} + \left((\tau_1c_{23} - \tau_2c_{24})\sin\tau_2y + (\tau_1c_{24} + \tau_2c_{23})\cos\tau_2y\right)e^{-\tau_1y} - \sum_{r=0}^{k}\frac{1}{r!}\left((a_{31}c_{15} - m_{3c_{16}})\sin m_3y + (a_{31}c_{16} + m_3c_{15})\cos m_3y\right)e^{-a_{31}y} - \sum_{r=0}^{k}\frac{1}{r!}\left((a_{32}c_{17} - m_3c_{18})\,sin\,m_3y + (a_{32}c_{18} + m_3c_{17})\,\cos m_3y\right)e^{-a_{32}y}\right)$$

$$G = n_1a_5e^{-n_1y} + ma_6e^{-my} + S_cv_0a_7e^{-S_cv_0y} + \sum_{r=0}^{k}\frac{a_8a_4}{r!}[m(n + r) + S_cv_0]e^{-[m(n+r)+S_cv_0]y}$$

$$H = S_cv_0e^{-S_cv_0y} + \varepsilon\left(\left(b_{11}S_cv_0 + b_9(S_cv_0y - 1)\right)e^{-S_cv_0y} + \sum_{r=0}^{k}\frac{1}{r!}((a_{31}b_1 - m_3b_2)\cos m_3y - (a_{31}b_2 + m_3b_1)\sin m_3y)e^{-(a_{31})y} + \sum_{r=0}^{k}\frac{1}{r!}((b_3a_{32} - b_4m_3)\cos m_3y - (b_4a_{32} + b_3m_3)\sin m_3y)e^{-a_{32}y} + \sum_{r=0}^{k}\frac{1}{r!}(b_5a_{34}e^{-a_{34}y} + b_7a_{33}e^{-a_{33}y}) + \sum_{r=0}^{k}\frac{a_{13}}{r!}a_{33}e^{-[m(n+r)+S_cv_0]y}\right)$$

$$L = \varepsilon\Bigg(b_{12}S_c v_0 e^{-S_c v_0 y} + \sum_{r=0}^{k}\frac{1}{r!}\big((a_{31}b_1 - m_3 b_2)\sin m_3 y + (a_{31}b_2 + m_3 b_1)\cos m_3 y\big)e^{-a_{31}y} + \sum_{r=0}^{k}\frac{1}{r!}\big((b_3 a_{32} - b_4 m_3)\sin m_3 y + (b_3 m_3 + b_4 a_{32})\cos m_3 y\big)e^{-(a_{32})y} + \sum_{r=0}^{k}\frac{1}{r!}(b_6 a_{34}e^{-a_{34}y} + b_8 a_{33}e^{-a_{33}y}) + b_{10}(S_c v_0 y - 1)e^{-S_c v_0 y}\Bigg)$$

$$K = (1+\varepsilon a_3)S_c v_0 e^{-S_c v_0 y} + \epsilon\Bigg(\sum_{r=0}^{k}\frac{a_4}{r!}[m(n+r)+S_c v_0]e^{-[m(n+r)+S_c v_0]y}(H\cos\omega t - L\sin\omega t)\Bigg)$$

$$P = \epsilon(H\sin\omega t + L\cos\omega t),\quad a = (me^{-my} + \epsilon A)^2 - B^2, b = 2B(me^{-my} + \epsilon A)$$

$$c = (me^{-my} + \epsilon A)^2 + \delta_1\big(G^2 - 2\epsilon FG + \epsilon^2(F^2 - E^2)\big) + \delta_2(K^2 - P^2 + 2IKP) - B^2 + \delta_3 Qme^{-my} + \epsilon\big((QR - ZS)\cos\omega t - (QS + ZR)\sin\omega t\big)$$

$$d = 2B(me^{-my} + \epsilon A) + 2\epsilon E(G - \epsilon F) + \delta_3 Zme^{-my} + \epsilon\big((QS + ZR)\cos\omega t + (QR - ZS)\sin\omega t\big)$$

where

$$R = c_1 me^{-my} + ((c_3 m_2 - c_4 m_3)\cos m_3 y - (c_3 m_3 + c_4 m_2)\sin m_3 y)e^{-m_2 y}$$

$$S = c_2 me^{-my} + ((c_3 m_2 - c_4 m_3)\sin m_3 y + (c_3 m_3 + c_4 m_2)\cos m_3 y)e^{-m_2 y}$$

$$a_{31} = m_2 + (n+r)m + S_c v_0, a_{32} = m_2 + (n+r-1)m + S_c v_0,$$

$$a_{33} = m(n+r) + S_c v_0, m(n+r+1) + S_c v_0$$

$$U = S_c v_0 e^{-S_c v_0 y} + \epsilon\Bigg(b_{11}S_c v_0 e^{-S_c v_0 y} + \sum_{r=0}^{k}\frac{1}{r!}((b_1 a_{31} - b_2 m_3)\cos m_3 y - (b_2 a_{31} + b_1 m_3)\sin m_3 y)e^{-(a_{31})y} + \sum_{r=0}^{k}\frac{1}{r!}b_5 a_{34}e^{-a_{34}y} + \sum_{r=0}^{k}\frac{1}{r!}((b_3 a_{32} - b_4 m_3)\cos m_3 y - (b_3 m_3 + b_4 a_{32})\sin m_3 y)e^{-a_{32}y} + \sum_{r=0}^{k}\frac{1}{r!}(b_7 a_{33} + a_{13}a_{34})e^{-a_{33}y} + b_9(S_c v_0 y - 1)e^{-S_c v_0 y}\Bigg)$$

$$V = \epsilon(b_{12}S_c v_0 e^{-S_c v_0 y} + \sum_{r=0}^{k}\frac{1}{r!}\big((b_1 a_{31} - b_2 m_3)\sin m_3 y + (b_1 m_3 + b_2 a_{31})\cos m_3 y\big)e^{-a_{31}y} + \sum_{r=0}^{k}\frac{1}{r!}((b_3 a_{32} - b_4 m_3)\sin m_3 y + (b_3 m_3 + b_4 a_{32})\cos m_3 y)e^{-a_{32}y} + \sum_{r=0}^{k}\frac{1}{r!}(b_6 a_{34}e^{-a_{34}y} + b_8 a_{33}e^{-a_{33}y}) + b_{10}(S_c v_0 y - 1)e^{-S_c v_0 y}$$

$$Q = (1+\varepsilon a_3)S_c v_0 e^{-S_c v_0 y} + \varepsilon\sum_{r=0}^{k}\frac{a_4}{r!}a_{33}e^{-a_{33}y} + \epsilon(U\cos\omega t - V\sin\omega t)$$

$$Z = \epsilon(V\cos\omega t + U\sin\omega t)$$

## 5. Results and discussion

Our analysis was carried out with parameter base values chosen as $Ha = 0.4, N = 0.6, \beta = -0.5, Gr = 5, \lambda = -0.6, \epsilon = 0.1, Pr = 0.71, Sc = 0.6, v_0 = 0.2, n = 2, V = 0.3$ unless otherwise. The graphical representation of our result was implemented by computer programme executed by Maple 2021. To be sure of our computations, we compared our result with existing results when certain conditions were imposed on the model. The results of our comparisons were displayed in Table 1. From this table, it is established that our results were in good agreement.

In Table 2, we displayed the effect flow governing parameters on the wall flow rate. The table shows that increase in heat generation decrease the skin friction and mass transfer rate while heat transfer rate increases whereas, the reverse is the case for increase in heat absorption. The effect of all other parameters on wall rate transfer were self-explanatory as displayed in the table. Using Pearson Correlation Coefficient analysis on the results displayed in Table 2, we observed that $\beta, \alpha, Gr$ and $Ha$ were all correlated, that is increase in these parameters brings about increase in skin friction but skin friction declines with increase in $\lambda$.

**Table 1** Comparison of average Nusselt number with some previous numerical results

| | **Nu** | | |
|---|---|---|---|
| | **Ra=10** | **Ra=100** | **Ra=1000** |
| Baytas and Pop [49] | 1.079 | 3.16 | 14.06 |
| Manole and Lage [50] | -------- | 3.12 | 13.64 |
| Moya *et al*. [51] | 1.065 | 2.80 | ------- |
| **Shohel and Roydon [47]** | 1.079 | 3.14 | 13.82 |
| Okedoye, Salawu and Asibor [16] | 1.0795 | 3.1431 | 13.7968 |
| Present Work | 1.0795 | 3.1431 | 13.7968 |

**Table 2** Rate of heat Transfer at the wall

| **Parameters** | $c_f$ | $Nu$ | $Sh$ | **Parameters** | $c_f$ | $Nu$ | $Sh$ |
|---|---|---|---|---|---|---|---|
| $\beta = -1.2$ | 10.5504 | 0.54011 | 0.13197 | $Gr = 0.5$ | 1.46469 | 0.56904 | 0.12753 |
| $\beta = -0.8$ | 10.8565 | 0.43947 | 0.14336 | $Gr = 1.0$ | 2.45778 | | |
| $\beta = 0.0$ | 11.4885 | 0.30773 | 0.16700 | $Gr = 2.0$ | 4.44397 | | |
| $\beta = 0.4$ | 32.7645 | 0.01655 | 0.45536 | $Gr = 4.0$ | 8.41635 | | |
| $\alpha = -0.5$ | 9.6711 | 0.93748 | 0.10712 | $Ha = 0.5$ | 1.24368 | | |
| $\alpha = -0.2$ | 10.2082 | 0.71475 | 0.11709 | $Ha = 1.0$ | 1.26448 | | |
| $\alpha = 0.2$ | 10.4023 | 0.56904 | 0.12753 | $Ha = 2.0$ | 1.42018 | | |
| $\alpha = 0.4$ | 10.5317 | 0.52245 | 0.13200 | $Ha = 4.0$ | 1.73067 | | |
| $\lambda = -1.5$ | 1.27648 | 0.56904 | 0.20941 | $v_0 = -2$ | -0.38050 | 0.01692 | -0.84350 |
| $\lambda = -0.8$ | 1.26838 | | 0.14573 | $v_0 = -1$ | -1.55850 | 0.01725 | -0.76490 |
| $\lambda = 1.2$ | 1.24525 | | -0.0362 | $v_0 = 1$ | 3.60115 | 0.01794 | 0.76801 |
| $\lambda = 3.0$ | 1.22444 | | -0.109 | $v_0 = 2$ | 3.44329 | 0.01830 | 1.29357 |

**Table 3** Interpretation of Table 2 using Pearson Correlation coefficient

| **Parameters** | $c_f$ | $Nu$ | $Sh$ |
|---|---|---|---|
| $\beta$ | 0.796308 | 0.967498 | -0.82963 |
| $\alpha$ | 0.952114 | 0.976097 | -0.99723 |
| Gr | 1.000000 | - | - |
| Ha | 0.994815 | - | - |
| $\lambda$ | -1.000000 | - | 0.985324 |

### 5.1. Entropy generation

Figure 2 represents the impact of heat generation parameter $\alpha$ versus entropy generation due to thermal irreversibility$\Gamma_\theta$. A larger estimation of $\alpha$ leads to an upsurge in the thermal force in the flow regime and as a result disorders in the system increase. Therefore $\Gamma_\theta$ is augmented. The outcome of $\Gamma_\theta$ for heat absorption $\beta$ and Suction $v_0$ is portrayed in Figure 3 and 4 respectively. It is noticed from both figures that larger estimation leads to reduction in $\Gamma_\theta$. Figure 5 is plotted to show the outcome of the entropy generation due to thermal irreversibility $\Gamma_\theta$ for the Grasshof number$G_r$. An intensification in $G_r$ clearly reduces the viscous force in the flow regime and as a result entropy rate reduces with$G_r$. Figure 6 is outlined to discuss the physical feature of Hartmann number $H_a$ on $\Gamma_u$ . The physically higher magnetic effect creates a stronger resistance in the liquid flow regime, which reduces the disorders in the system. Thus, entropy rate, $\Gamma_\theta$ is reduced. The increase in the viscous irreversibility distribution ratio $\delta 1$ reduces $\Gamma_\theta$ as depicted in Figure 7.

The effect of heat generation parameter$\alpha$, heat absorption$\beta$, reactivity parameter $\lambda$ and diffusive irreversibility distribution ratio $\delta 2$ on entropy generation due to diffusivity irreversibility $\Gamma_d$ is depicted in Figure 8-11 respectively. From the figures it clearly seen that the intensification of $\alpha, \beta, \lambda$ and $\delta 2$ the reduces the entropy generation due to diffusivity irreversibility of the system. Figure 12 depicts the outcome of the entropy generation $E_G$ versus heat generation parameter$\alpha$. Clearly $E_G$ reduces with $\alpha$.

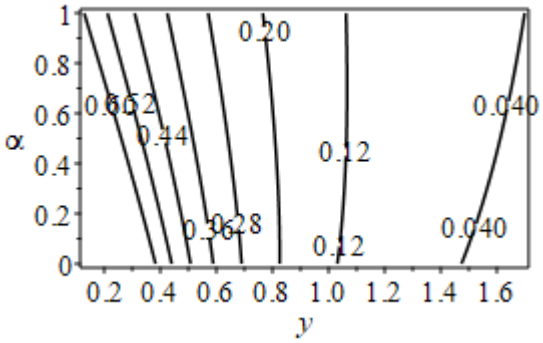


**Figure 2** Effect of radiation parameter on $\Gamma_{n,\theta}$

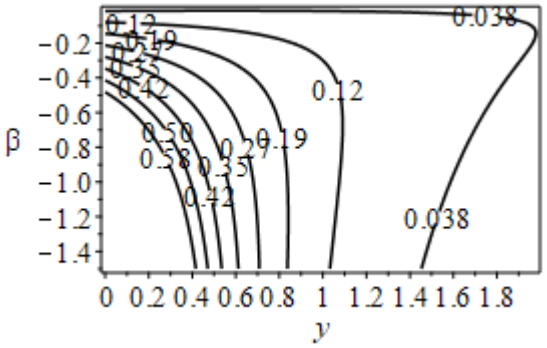


**Figure 3** Effect of heat generation on $\Gamma_{n,\theta}$

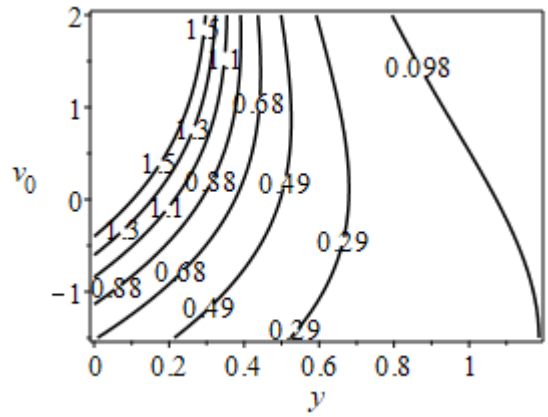


**Figure 4** Effect of suction parameter on $\Gamma_\theta$

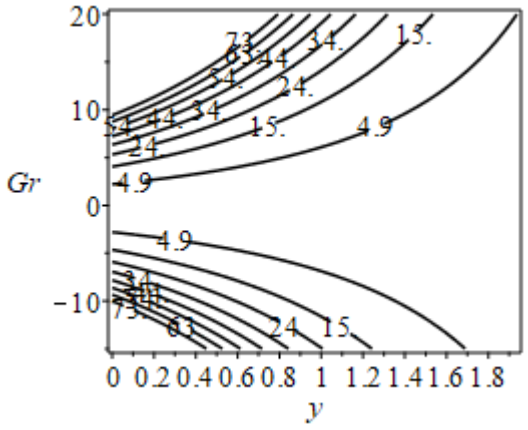


**Figure 5** Nature of buoyancy petameter on $\Gamma_u$

It is noticed from Figure 13 that $E_G$ reduces with $\beta$. The intensification in $H_a$ leads to an upsurge in the viscous force in the flow regime and as a result disorders in the system increase. Therefore $E_G$ is augmented as seen in Figure 14. It is observed in Figure 15-17 that $E_G$ is augmented when $\delta 1, N$ and $v_0$ was intensified.

### 5.2. Bejan Number

Figure 18-25 describe the effect of $B_e$ on heat generation parameter $\alpha$, heat absorption β, Grasshof number $Gr$, Hatmann number $Ha$, Radiation parameter $N$, Suction $v_0$, Thermal irreversisibilty distribution ratio $\delta 3$ and surface velocity $V$ respectively. The effect of these parameters was as shown. Clearly, it is observed from Fig. 22 that the presence of Hartmann number has an increasing effect on $Be$. Figure 24 depicts the behavior of $Be$ for different values

of suction/Injection. And in Figure 25, we show the impact of surface velocity on Bejan number. The Figure revealed that as suction increase, there is increase in heat transfer irreversibility and when injection increases on the medium, the heat transfer irreversibility decreases. From the other Figures, it is clear that the variation in heat generation parameter $\alpha$, heat absorption $\beta$, Grasshof number $G_r$, Radiation parameter $N$and thermal irreversibility distribution ratio $\delta 3$ reduces $Be$.

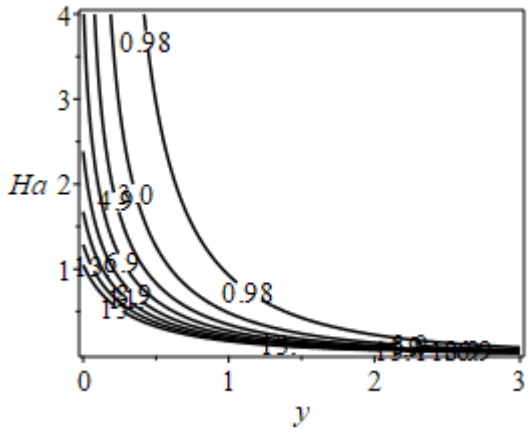


**Figure 6** Nature of Hartmann number $H_a$ on $\Gamma_u$

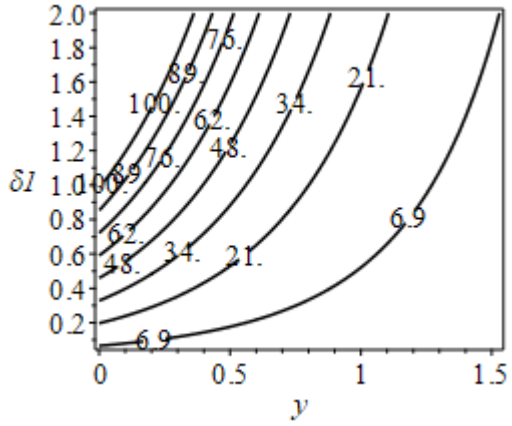


**Figure 7** Nature of viscous irreversibility ratio on $\Gamma_u$

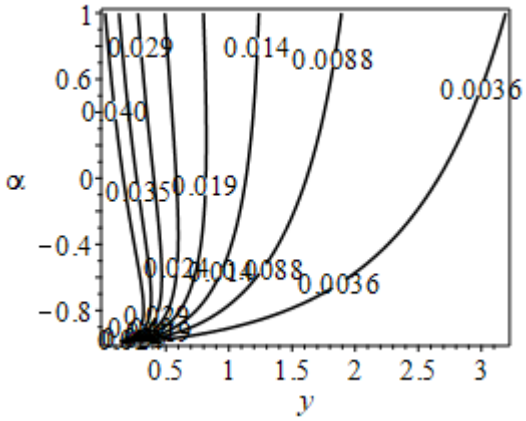


**Figure 8** Behaviour of radiation on $\Gamma_d$

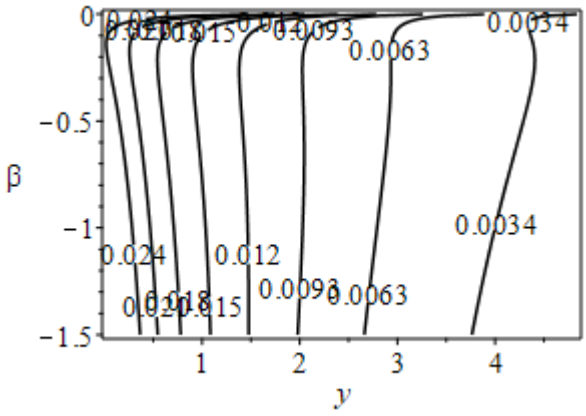


**Figure 9** Behaviour of heat generation on $\Gamma_d$

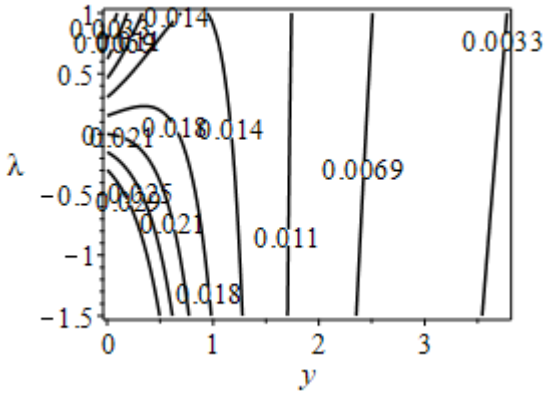


**Figure 10** Behaviour of reactivity parameter on $\Gamma_d$

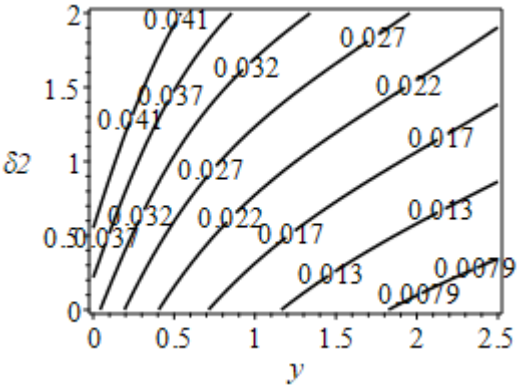


**Figure 11** Behaviour of viscous irreversibility ration on $\Gamma_d$

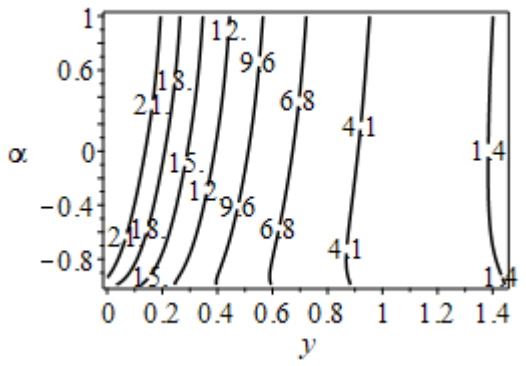


**Figure 12** Behaviour of radiation parameter on $E_G$

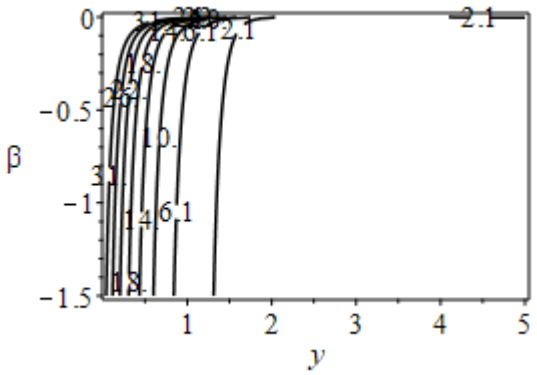


**Figure 13** Behaviour of heat generation parameter on $E_G$

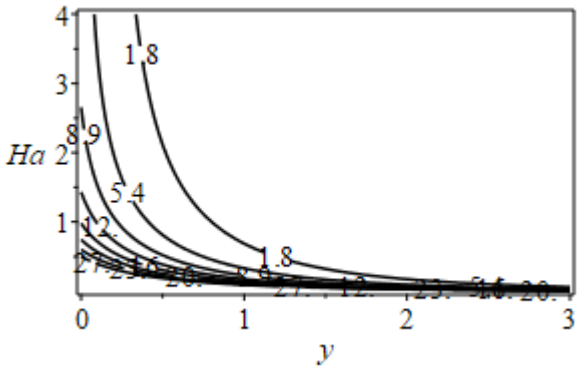


**Figure 14** Behaviour of Hartmann number on $E_G$

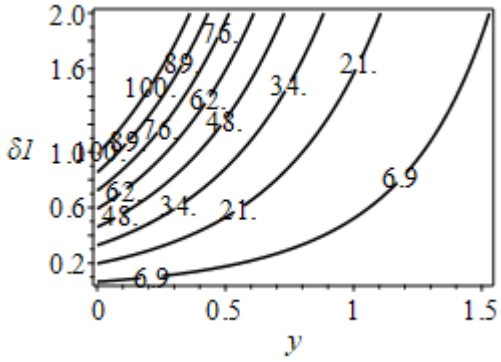


**Figure 15** Behaviour of viscous irreversibility ration on $E_G$

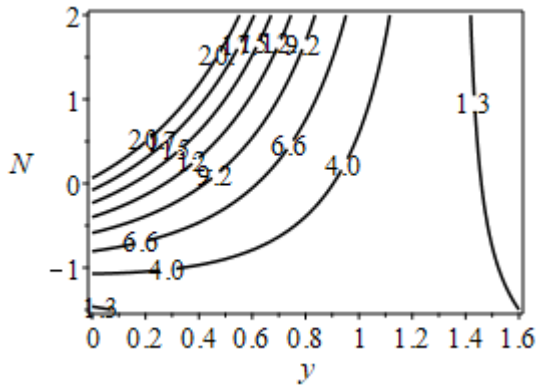


**Figure 16** Behaviour of Buoyancy ratio on $E_G$

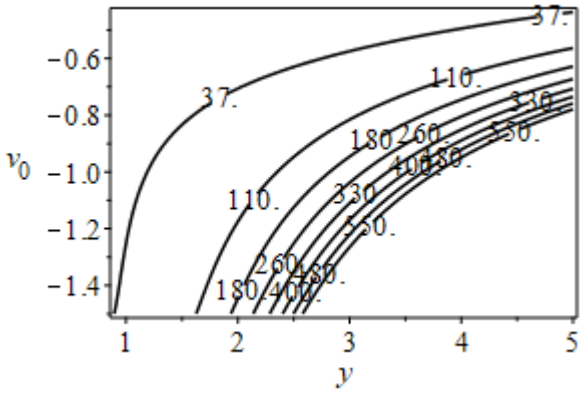


**Figure 17** Behaviour of suction parameter on $E_G$

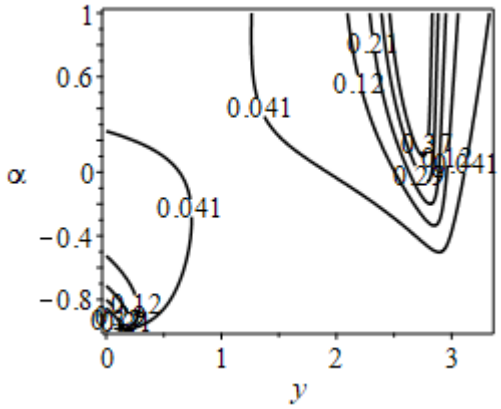


**Figure 18** Effect of radiation on $B_e$

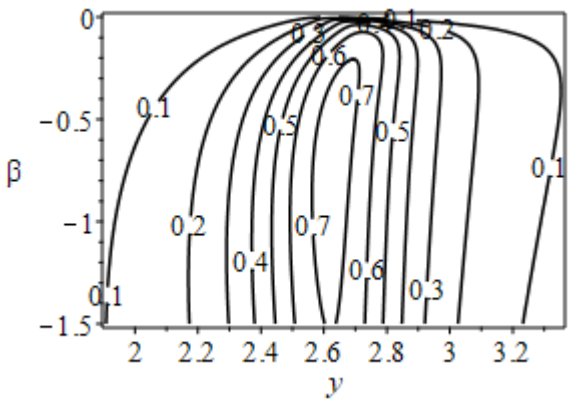


**Figure 19** Effect of heat generation on $B_e$

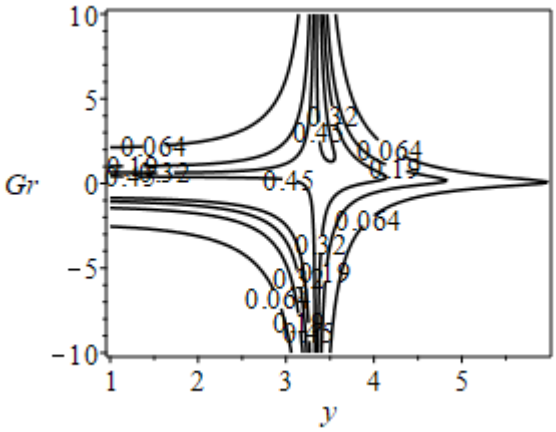


**Figure 20** Effect of mass Grashof number on $B_e$

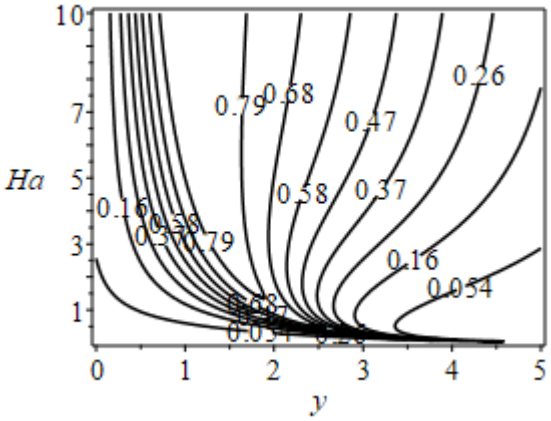


**Figure 21** Effect of Hartmann on $B_e$

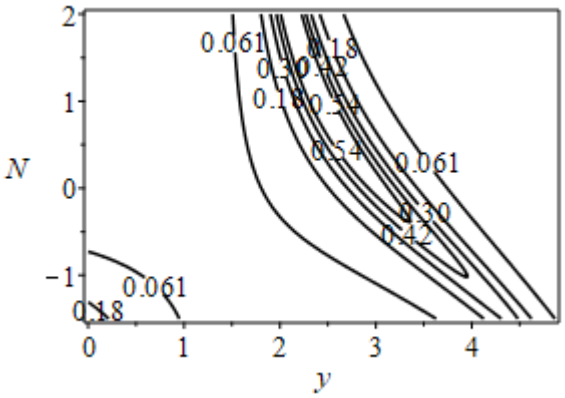


**Figure 22** Effect of Buoyancy ration on $B_e$

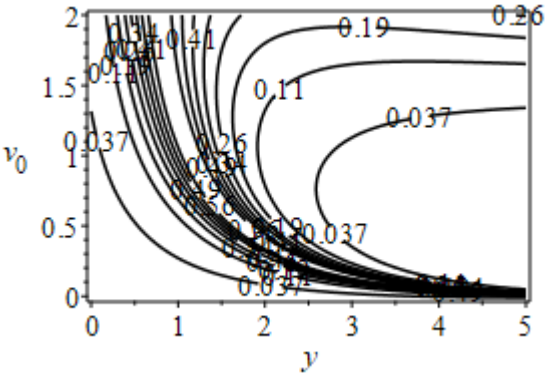


**Figure 23** Effect of suction parameter on $B_e$

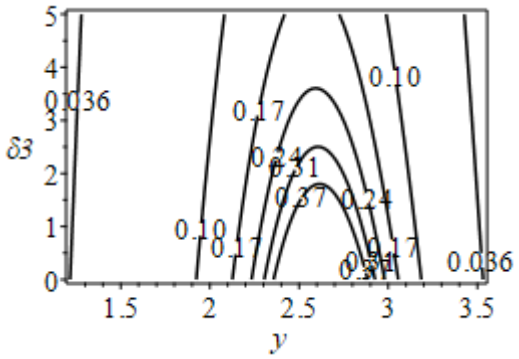


**Figure 24** Effect of diffusivity irreversibility ratio on $B_e$

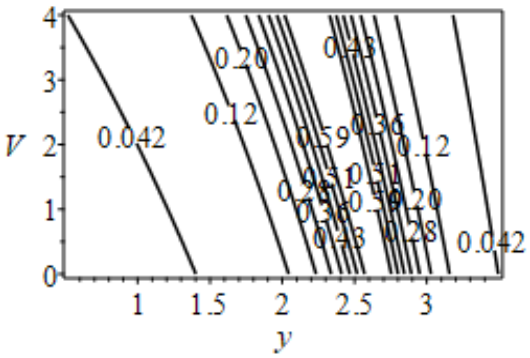


**Figure 25** Effect of surface velocity on $Be$

## Appendix

*Appendix A*

$$m = \frac{Prv_0 + \sqrt{Pr^2 v_0^2 - 4Pr(1+\alpha)\beta}}{2(1+\alpha)}, m_1 = \frac{Prv_0 + \sqrt{Pr^2 v_0^2 - 4Pr(1+\alpha)(\beta - \frac{i\omega}{4})}}{2(1+\alpha)}$$

$$n_1 = \frac{v_0 + \sqrt{v_0^2 + 4Ha}}{2}, \tau = \frac{v_0 + \sqrt{v_0^2 + 4\left(Ha + \frac{i\cdot\omega}{4}\right)}}{2}, a_1 = 1 - a_2, a_3 = -\sum_{r=0}^{k} \frac{a_4}{r!},$$

$$a_2 = -\frac{Prv_0}{(1+\alpha)m^2 - mPrv_0 + Pr\left(\beta - \frac{i\omega}{4}\right)}, a_4 = -\frac{\lambda Sc}{m(n+r)(m(n+r) + S_c v_0)},$$

$$a_5 = 2 - a_6 - a_7 - a_8, a_6 = -\frac{GrN}{m^2 - mv_0 - Ha}, a_7 = -\frac{Gr\left(1 - \varepsilon\sum_{r=0}^{k}\frac{a_4}{r!}\right)}{S_c^2 v_0^2 - S_c v_0^2 - Ha}$$

$$a_8 = -\frac{\varepsilon Gr}{(m(n+r) + S_c v_0)^2 - v_0(m(n+r) + S_c v_0) - Ha}$$

$$a_{15} = -(a_9 + a_{10} + a_{11} + a_{12} + a_{13} + a_{14}), \qquad a_{13} = \frac{S_c v_0^2}{m(n+r)},$$

$$a_9 = \frac{\lambda Sc a_1}{(m_1 + (n+r)m + S_c v_0)(m_1 + (n+r)m)}, a_{14} = -\frac{\left(v_0^2(1+\varepsilon a_3) - \frac{i\omega\lambda}{4}\right)}{S_c v_0},$$

$$a_{10} = \frac{\lambda Scn a_1}{(m_1 + (n+r-1)m + S_c v_0)(m_1 + (n+r-1)m)}$$

$$a_{11} = \frac{\lambda Sc a_2}{(m(n+r+1) + S_c v_0)(m(n+r+1))}, a_{12} = \frac{n\lambda Sc a_2}{\left((n+r)m + S_c v_0\right)((n+r)m)}$$

$$a_{25} = 1 - a_{16} - a_{17} - a_{18} - a_{19} - a_{20} - a_{21} - a_{22} - a_{23} - a_{24}$$

$$a_{16} = -\frac{v_0 a_5}{n_1^2 - v_0 n_1 - \left(Ha + \frac{i\cdot\omega}{4}\right)}, \quad a_{17} = -\frac{(v_0 a_6 + GrNa_2)}{m^2 - v_0 m - \left(Ha + \frac{i\cdot\omega}{4}\right)}$$

$$a_{18} = \frac{\varepsilon Gr a_{11}}{S_c^2 v_0^2 - S_c v_0^2 - \left(Ha + \frac{i \cdot \omega}{4}\right)}, a_{19} = \frac{a_7 + Gr(1 + \varepsilon a_5) + a_{16}(-2Scv_0 + v_0)}{S_c^2 v_0^2 - S_c v_0^2 - \left(Ha + \frac{i \cdot \omega}{4}\right)}$$

$$a_{24} = \frac{Ha + v_0 - \frac{i \cdot \omega}{4}}{\left(Ha + \frac{i \cdot \omega}{4}\right)}, a_{20} = -\frac{GrNa_1}{m_1^2 - m_1 v_0 - \left(Ha + \frac{i \cdot \omega}{4}\right)}$$

$$a_{21} = \frac{\varepsilon Gr a_6}{(m_1 + (n+r)m + S_c v_0)^2 - v_0(m_1 + (n+r)m + S_c v_0) - \left(Ha + \frac{i \cdot \omega}{4}\right)}$$

$$a_{22} = \frac{\varepsilon Gr a_7}{(m_1 + (n+r-1)m + S_c v_0)^2 - v_0(m_1 + (n+r-1)m + S_c v_0) - \left(Ha + \frac{i \cdot \omega}{4}\right)}$$

$$a_{23} = \frac{\varepsilon Gr(v_0 a_8 a_4 + a_9 + a_{10})}{[m(n+r) + S_c v_0]^2 - v_0[m(n+r) + S_c v_0] - \left(Ha + \frac{i \cdot \omega}{4}\right)}$$

*Appendix B*

**Table 4** Contour Values for various values of Parameters

| | **Contour Values** | | | | | | | | | **Range** |
|---|---|---|---|---|---|---|---|---|---|---|
| $\beta$ | $\Gamma_{n,\theta}$ | 0.04 | 0.12 | 0.19 | 0.27 | 0.35 | 0.42 | 0.50 | 0.58 | 0.54 |
| | $\Gamma_{n,u}$ | 1.50 | 4.60 | 7.70 | 11.00 | 14.00 | 17.00 | 20.00 | 23.00 | 21.50 |
| | $\Gamma_{n,d}$ | 1.50 | 4.60 | 7.70 | 11.00 | 14.00 | 17.00 | 20.00 | 23.00 | 21.50 |
| | $E_G$ | 2.10 | 6.10 | 10.00 | 14.00 | 18.00 | 22.00 | 26.00 | 31.00 | 28.90 |
| | $Be$ | 0.05 | 0.14 | 0.23 | 0.31 | 0.40 | 0.49 | 0.57 | 0.66 | 0.61 |
| $Gr$ | $\Gamma_{n,\theta}$ | 0.86 | 2.60 | 4.30 | 6.00 | 7.80 | 9.50 | 11.00 | 13.00 | 12.14 |
| | $\Gamma_{n,u}$ | 6.00 | 18.00 | 30.00 | 42.00 | 54.00 | 66.00 | 78.00 | 90.00 | 84.00 |
| | $\Gamma_{n,d}$ | 0.00 | 0.01 | 0.01 | 0.02 | 0.02 | 0.03 | 0.03 | 0.04 | 0.03 |
| | $E_G$ | 12.00 | 37.00 | 62.00 | 87.00 | 110.00 | 140.00 | 160.00 | 190.00 | 178.00 |
| | $Be$ | 0.03 | 0.09 | 0.15 | 0.21 | 0.27 | 0.33 | 0.39 | 0.45 | 0.42 |
| $Ha$ | $\Gamma_{n,\theta}$ | 0.06 | 0.18 | 0.29 | 0.41 | 0.53 | 0.65 | 0.76 | 0.88 | 0.82 |
| | $\Gamma_{n,u}$ | 2.20 | 6.70 | 11.00 | 16.00 | 20.00 | 24.00 | 29.00 | 33.00 | 30.80 |
| | $\Gamma_{n,d}$ | 0.00 | 0.01 | 0.01 | 0.01 | 0.02 | 0.02 | 0.02 | 0.03 | 0.02 |
| | $E_G$ | 2.30 | 6.90 | 12.00 | 16.00 | 21.00 | 25.00 | 30.00 | 35.00 | 32.70 |
| | $Be$ | 0.06 | 0.16 | 0.27 | 0.38 | 0.49 | 0.59 | 0.70 | 0.81 | 0.75 |
| $N$ | $\Gamma_{n,\theta}$ | 0.06 | 0.17 | 0.28 | 0.40 | 0.51 | 0.62 | 0.74 | 0.85 | 0.79 |
| | $\Gamma_{n,u}$ | 1.30 | 4.00 | 6.60 | 9.20 | 12.00 | 15.00 | 17.00 | 20.00 | 18.70 |
| | $\Gamma_{n,d}$ | 0.00 | 0.01 | 0.01 | 0.01 | 0.02 | 0.02 | 0.03 | 0.03 | 0.03 |
| | $E_G$ | 1.30 | 3.80 | 6.30 | 8.80 | 11.00 | 14.00 | 16.00 | 19.00 | 17.70 |
| | $Be$ | 0.04 | 0.11 | 0.19 | 0.26 | 0.34 | 0.41 | 0.48 | 0.56 | 0.52 |
| $\lambda$ | $\Gamma_{n,\theta}$ | 0.03 | 0.08 | 0.13 | 0.18 | 0.23 | 0.28 | 0.33 | 0.38 | 0.35 |

| | | | | | | | | | | |
|---|---|---|---|---|---|---|---|---|---|---|
| | $\Gamma_{n,u}$ | 1.30 | 3.80 | 6.30 | 8.90 | 11.00 | 14.00 | 16.00 | 19.00 | 17.70 |
| | $\Gamma_{n,d}$ | 0.00 | 0.01 | 0.01 | 0.01 | 0.02 | 0.02 | 0.03 | 0.03 | 0.03 |
| | $\mathrm{E}_G$ | 1.20 | 3.70 | 6.10 | 8.50 | 11.00 | 13.00 | 16.00 | 18.00 | 16.80 |
| | $Be$ | 0.04 | 0.12 | 0.20 | 0.28 | 0.36 | 0.44 | 0.52 | 0.60 | 0.56 |
| $v_0$ | $\Gamma_{n,\theta}$ | 0.10 | 0.29 | 0.49 | 0.68 | 0.88 | 1.10 | 1.30 | 1.50 | 1.40 |
| | $\Gamma_{n,u}$ | 130.0 | 390.0 | 640.0 | 900.0 | 1200.0 | 1400.0 | 1700.0 | 1900.0 | 1770.0 |
| | $\Gamma_{n,d}$ | 2.00 | 6.20 | 10.00 | 14.00 | 19.00 | 23.00 | 27.00 | 31.00 | 29.00 |
| | $\mathrm{E}_G$ | 37.00 | 110.00 | 180.00 | 260.00 | 330.00 | 400.00 | 480.00 | 550.00 | 513.00 |
| | $Be$ | 0.04 | 0.11 | 0.19 | 0.26 | 0.34 | 0.41 | 0.49 | 0.56 | 0.52 |
| $V$ | $\Gamma_{n,\theta}$ | 0.10 | 0.31 | 0.52 | 0.73 | 0.93 | 1.10 | 1.30 | 1.60 | 1.50 |
| | $\Gamma_{n,u}$ | 1.00 | 3.10 | 5.10 | 7.10 | 9.20 | 11.00 | 13.00 | 15.00 | 14.00 |
| | $\Gamma_{n,d}$ | 0.00 | 0.01 | 0.01 | 0.02 | 0.02 | 0.02 | 0.03 | 0.03 | 0.03 |
| | $\mathrm{E}_G$ | 1.30 | 3.80 | 6.30 | 8.80 | 11.00 | 14.00 | 16.00 | 19.00 | 17.70 |
| | $Be$ | 0.04 | 0.12 | 0.20 | 0.28 | 0.36 | 0.43 | 0.51 | 0.59 | 0.55 |
| $\alpha$ | $\Gamma_{n,\theta}$ | 0.04 | 0.12 | 0.20 | 0.28 | 0.36 | 0.44 | 0.52 | 0.60 | 0.56 |
| | $\Gamma_{n,u}$ | 1.30 | 3.80 | 6.30 | 8.80 | 11.00 | 14.00 | 16.00 | 19.00 | 17.70 |
| | $\Gamma_{n,d}$ | 0.00 | 0.01 | 0.01 | 0.02 | 0.02 | 0.02 | 0.03 | 0.03 | 0.03 |
| | $\mathrm{E}_G$ | 1.30 | 3.90 | 6.50 | 9.10 | 12.00 | 14.00 | 17.00 | 20.00 | 18.70 |
| | $Be$ | 0.03 | 0.08 | 0.14 | 0.19 | 0.24 | 0.30 | 0.35 | 0.41 | 0.38 |
| n | $\Gamma_{n,\theta}$ | 0.10 | 0.31 | 0.52 | 0.73 | 0.93 | 1.10 | 1.30 | 1.60 | 1.50 |
| | $\Gamma_{n,u}$ | 1.30 | 3.90 | 6.40 | 9.00 | 12.00 | 14.00 | 17.00 | 19.00 | 17.70 |
| | $\Gamma_{n,d}$ | 0.00 | 0.01 | 0.02 | 0.02 | 0.03 | 0.04 | 0.05 | 0.05 | 0.05 |
| | $\mathrm{E}_G$ | 1.40 | 4.30 | 7.10 | 9.90 | 13.00 | 16.00 | 18.00 | 21.00 | 19.60 |
| | $Be$ | 0.01 | 0.03 | 0.04 | 0.06 | 0.07 | 0.09 | 0.11 | 0.12 | 0.11 |

## 6. Conclusion

The analysis of Entropy Generation in Unsteady MHD Convective Flow past a Flat Porous Oscillating Plate with Suction or Injection is investigated. Some key outcomes of the analysis are as follows:

- The Entropy generation due to thermal irreversibility $\Gamma_\theta$ enhances with increasing value of $\lambda$, while opposite behaviour is seen for $\beta$ and $v_0$.
- The Entropy generation due to viscous irreversibility $\Gamma_u$ decreases with the increase in $G_r$ and $H_a$.
- Entropy generation due to diffusive irreversibility $\Gamma_d$ reduces with increment in the value of $\beta$ and $\lambda$.
- The Bejan number $\mathrm{B}_e$ reduces as the result of thermal irreversibility distribution ratio $\delta 3$ and radiation parameter $N$ increase.
- Entropy generation $\mathrm{E}_G$ and Bejan numbers $\mathrm{B}_e$ are improved by the Hatmann Number $H_a$.
- Entropy generation $\mathrm{E}_G$ has an increasing effect for radiation parameter $N$

## Compliance with ethical standards

*Acknowledgments*

The management of Covenant University is appreciated and thanked by the writers for providing conducive environment and research facilities. We also appreciate the unnamed referees' helpful comments, which helped to improve the final product.

*Disclosure of conflict of interest*

The authors declare that they have no known competing financial interests or personal relationships that could have appeared to influence the work reported in this paper.

## References

[1] Menni, Y, A. J. Chamakha and A. Azzi, "Nanofluid transport in porous media: a review," Special Topics & Reviews in Porous Media: An International Journal, vol. 10, no. 1, pp 49-64, 2019.

[2] Saffman, P.G: On the boundary condition at the surface of a porous medium, Studies App. Math. 50 (1971) 93-101.

[3] Hayat, Z. Hussain, Z, Alsaedi, A and Ahmad, B. Heterogeneous-homogeneous reactions and melting heat transfer effects in flow with carbon nanotubes, J. Mol. Liq. 220 (2016) 200-207.

[4] Krishnamurthy, M.R, Gireesha, B.J, Gorla, R.S.R. and B.C. Prasannakumara, Suspended Particle effect on slip flow and melting heat transfer of nanofluid over a stretching sheet embedded in a porous medium in the presence of nonlinear thermal radiation, J. Nanofluids 5 (2016) 502-510.

[5] Sharma, P.R and Singh, G: "Unsteady MHD free convective flow and and heat transfer along a vertical porous plate withvariable suction and internal heat generation," International Journal of Applied Mathematics and Mechanics, vol. 4, no. 5, pp. 1–8, 2008.

[6] Singh, P and Gupta, C.B, "MHD free convective flow of viscous fluid through a porous medium bounded by an oscillating porous plate in slip flow regime with mass transfer," Indian Journal of Theoretical Physics, vol. 53, no. 2, pp. 111–120, 2005.

[7] Haroun, N.A, P. Sibanda, P, Mondal, S, Motsa, S.S; On unsteady MHD mixed convection in a nanofluid due to a stretching/shrinking surface with suction/injection using the spectral relaxation method, Bound. Value Probl. 2015 (1) (2015) 24.

[8] Vaidya, H., Rajashekhar, C., Manjunatha, G., Wakif, A., Prasad, K. V., Animasaun, I. L., & Shivaraya, K. (2021). Analysis of entropy generation and biomechanical investigation of MHD Jeffery fluid through a vertical non-uniform channel. Case Studies in Thermal Engineering, 28, 101538. https://doi.org/10.1016/j.csite.2021.10153

[9] Ullah, I., Shafie, S., & Khan, I. (2017). Effects of slip condition and Newtonian heating on MHD flow of Casson fluid over a nonlinearly stretching sheet saturated in a porous medium. Journal of King Saud University, 29, 250–259. https://doi.org/10.1016/j.jksus. 2016.05.003

[10] Krishnamurthy, M. R., Prasannakumara, B. C., Gireesha, B. J., & Gorla, R. S. R. (2016). Effect of chemical reaction on MHD boundary layer flow and melting heat transfer of Williamson nanofluid in porousmedium. Engineering Science and Technology, an International Journal, 19, 53–61.

[11] Abbas, Z., Naveed, M., Hussain, M., & Salamat, N. (2020). Analysis of entropy generation for MHD flow of viscous fluid embedded in a vertical porous channel with thermal radiation. Alexandria Engineering Journal, 59, 3395–3405.

[12] Makinde, O.D and Aziz, A: "MHD mixed convection from a vertical plate embedded in a porous medium with a convective boundary condition," International Journal of Thermal Sciences, vol. 49, no. 9, pp. 1813–1820. 2010.

[13] Okedoye A. M. Salawu S. O.: Unsteady oscillatory MHD boundary layer flow past a moving plate with mass transfer and binary chemical reaction. Springer Nature Switzerland, SN Applied Sciences (2019) 1:1586 https://doi.org/10.1007/s42452-019-1463-7.

[14] A.M. Okedoye and S.O. Salawu (2019). Effect of nonlinear radiative heat and mass transfer on MHD flow over a stretching surface with variable conductivity and viscosity. Journal of the Serbian Society for Computational Mechanics, 13(2), 87-104.

[15] A.M. Okedoye and S.O. Salawu (2020): Transient Heat and Mass Transfer of Hydro magnetic Effects on the Flow Past a Porous Medium with Movable Vertical Permeable sheet. Int. J. of Applied Mechanics and Engineering, 2020, vol.25, No.4, pp.175-190 DOI: 10.2478/ijame-2020-0057.

[16] Akindele M. Okedoye, Sulyman O. Salawu and Raphael E. Asibor (2021): A convective MHD double diffusive flow of a binary mixture through an isothermal and porous moving plate with activation energy. Computational Thermal Sciences – 13(5):45–60 (2021). Begell House, Inc. www.begellhouse.com.

[17] Panya, A.L, Akeyemi, A.O and Okedoye, A.M. (2023): MHD Darcy-Forchheimer Slip Flow in a Porous Medium with Variable Thermo-Physical Properties. International Journal of Mechanical Technology. Vol 10, issue 2, pp: (30-42), ISSN 2348-7593. DOI:https://doi.org/10.5281/zenodo.7646344.

[18] Bejan, A. Entropy generation minimization, 2nd ed. Boca Raton: CRC Press. 1996

[19] Bejan, A. (1980). Second law analysis in heat transfer. Energy, 5, 720– 732. https://doi.org/10.1016/0360-5442(80)90091-2.

[20] Qing, J, Bhatti, M.M, Abbas, M.A, Rashidi, M.M and Ali ME-S, Entropy generation on MHD Casson nanofluid flow over a porous stretching/shrinking surface, Entropy 18 (2016) 123 (14 pages).

[21] Ajibade, A.O, Jha, B.K and Omame, A. Entropy generation under the effect of suction/injection. Applied Mathematical Modelling. 35(2011) 4630-4646. Doi:10.1016/j.apm.2011.03.027.

[22] Shit, G.C, Haldar, R and Mandal, S., Entropy generation on MHD flow and convective heat transfer in a porous medium of exponentially stretching surface saturated by nanofluids, Advanced Powder Technology (2017), http://dx.doi.org/10.1016/j.apt.2017.03.023

[23] Rashidi, M.M.; Bagheri, S.; Momoniat, E.; Freidoonimehr, N., Entropy analysis of convective MHD flow of third grade non-Newtonian fluid over a stretching sheet, Ain Shams Engineering Journal (2015), http://dx.doi.org/10.1016/j.asej.2015.08.012.

[24] Farooq, U, Afridi, M.I, Qasim, M and Lu, D.C.; Transpiration and viscous dissipation effects on entropy generation in hybrid nanofluid flow over a nonlinear radially stretching disk, Entropy 20 (9) (2018) 668.

[25] Nayak, M. K., Mabood, F., Dogonchi, A. S., & Khan,W. A. (2020). Electromagnetic flow of SWCNT/MWCNT suspensions with optimized entropy generation and cubic auto catalysis chemical reaction. International Communications in Heat and Mass Transfer, 120, 104996. https://doi.org/10.1016/j.icheatmasstransfer.2020.104996.

[26] Khan, M. I., & Alzahrani, F. (2020). Entropy-optimized dissipative flow of Carreau–Yasuda fluid with radiative heat flux and chemical reaction. The European Physical Journal, 135, 516. https://doi.org/10 .1140/epjp/s13360-020-00532-3

[27] Bianco, V, Nardini, S and Manca, O. Enhancement of heat transfer and entropy generation analysis of nanofluids turbulent convection flow in square sectiontubes. Nanoscale Research Letters, Vol. 6 no.1 article 252, 2011.

[28] Al-Zaharnah, I.T.; Yilbas, B.S. Thermal analysis in pipe flow: influence of variable viscosity on entropy generation. Entropy 2004, 6, 344–363.

[29] Abbas, Z., Naveed, M., Hussain, M., & Salamat, N. (2020). Analysis of entropy generation for MHD flow of viscous fluid embedded in a vertical porous channel with thermal radiation. Alexandria Engineering Journal, 59, 3395–3405. https://doi.org/10.1016/j.aej.2020.0 5.019

[30] Tayebi, T., Öztop, H. F., & Chamkha, A. J. (2020). Natural convection and entropy production in hybrid nanofluid filled-annular elliptical cavity with internal heat generation or absorption. Thermal Science and Engineering Progress, 19, 100605. https://doi.org/10.101 6/j.tsep.2020.100605.

[31] Avellaneda, J. M., Bataille, F., Toutant, A., & Flamant, G. (2020). Variational entropy generation minimization of a channel flow: Convective heat transfer in a gas flow. International Journal of Heat and Mass Transfer, 160, 120168. https://doi.org/10.1016/j.ijheatmasstr ansfer.2020.120168.

[32] Hayat, T., Shah, F., & Alseadi, A. (2020). Cattaneo–Christov double diffusions and entropy generation in MHD second grade nanofluid flow by a Riga wall. International Communications in Heat and Mass Transfer, 119, 104824. https://doi.org/10.1016/j.icheatmasstransf er.2020.104824

[33] Ramesh, K., Khan, S. U., Jameel, M., Khan, M. I., Chu, Y.-M., & Kadry, S. (2020). Bioconvection assessment in Maxwell nanofluid configured by a Riga surface with nonlinear thermal radiation and activation energy. Surface Interfaces, 21, 100749. https://doi.org/10.1 016/j.surfin.2020.100749.

[34] Waqas, M. (2020). A mathematical and computational framework for heat transfer analysis of ferromagnetic non-Newtonian liquid subjected to heterogeneous and homogeneous reactions. Journal of Magnetism and Magnetic Materials, 493, 165646. https://doi.org/ 10.1016/j.jmmm.2019.165646.

[35] Khan, M. I., & Alzahrani, F. (2021). Free convection and radiation effects in nanofluid (silicon dioxide and molybdenum disulfide) with second order velocity slip, entropy.

[36] Sahin, Z.A. Entropy generation in turbulent liquid flow through a smooth duct subjected to constant wall temperature. Int. J. Heat Mass Transfer 2000, 43, 1469–1478.

[37] Sahin, Z.A. Entropy generation and pumping power in a turbulent fluid flow through a smooth pipe subjected to constant heat flux. Exergy, an International Journal 2002, 2, 314–321.

[38] Makinde, O.D and Osalusi, E. (2005): Second Law Analysis of Laminar Flow in a Channel Filled With Saturated Porous Media. Entropy ISSN 1099-4300, 7[2], 148-160.

[39] Hirschfelder, J. O.; Curtis, C. F.; Bird, R. B. Molecular Theory of Gases and Liquids. Wiley: New York, 1954.

[40] Prigogine, I. Etude thermodynamique des processus irréversibles, 4th edition, Liège:Desoer, 1967.

[41] Magherbi Mourad, Abbassi Hassen, Hidouri Nejib, Ben Brahim Ammar (2006): Second law analysis in convective heat and mass transfer Entropy 2006, 8[1], 1-17. ISSN 1099-4300, www.mdpi.org/entropy/

[42] Biringen, S., Danabasoglu, G. Computation of convective flow with gravity modulation in rectangular cavities. J. Thermophys. 1990, 4, 357–365.

[43] Ogunseye, H., & Okoya, S. S; Criticality and thermal explosion in the flow of reactive viscous third grade fluid flow in a cylindrical pipe with surface cooling. Journal of the Nigerian Mathematical Society, 2017, 36(2), 399–418.

[44] A. M. OKEDOYE AND P. O. OGUNNIYI. MHD Boundary Layer Flow past a Moving Plate with Mass Transfer and Binary Chemical Reaction. Journal of the Nigerian Mathematical Society, 38, Issue 1, pp. 89-121, 2019.

[45] Messhiha S.A.S., Laminar Boundary Layers in Oscillatory Flow along an Infinite Flat Plate with Variable suction, Proc. Camb. Phil. Soc. 62 329-337, 1966.

[46] M. J. Lighthill, The response of laminar skin friction and heat transfer to fluctuations in the stream velocity, proceeding of the royal society of London A224, 1-23 1954.

[47] Shohel, M and Roydon, A. F. Analysis of mixed convection-radiation interaction in a vertical channel: entropy generation, Exergy, an International Journal, 2002, 2, 330-339.

[48] Tasnim, H. S; Shohel, M. Entropy generation in a vertical concentric channel with temperature dependent viscosity, Int. Comm. Heat Mass Transfer, 2002, 29 (7), 907-918.

[49] Baytas, A.C. and Pop, I. (1999), "Free convection in oblique enclosures filled with a porous medium", International Journal of Heat and Mass Transfer, Vol. 42, pp. 1047-1057.

[50] Manole, D.M. and Lage, J.L. (1992), "Numerical benchmark results for natural convection in a porous medium cavity", ASME Conference, Heat and Mass Transfer in Porous Media, HTD, Vol. 216, pp. 55-60

[51] Moya, S.L., Ramos, E. and Sen, M. (1987), "Numerical study of natural convection in a tilted rectangular porous material", International Journal of Heat and Mass Transfer, Vol. 30 No. 4, pp. 741-756